

Modern Physics Letters A
 © World Scientific Publishing Company

PANCHROMATIC STUDIES OF DISTANT CLUSTERS OF GALAXIES

Ricardo Demarco and Holland C. Ford

*Department of Physics and Astronomy, Johns Hopkins University, 3400 N. Charles Str.,
 Baltimore, MD 21218, USA
 demarco@pha.jhu.edu*

Piero Rosati

*ESO-European Southern Observatory, Karl-Schwarzschild Str. 2,
 Garching b. München, D-85748, Germany*

Received 5 May 2005

High redshift ($z \gtrsim 1$) clusters are ideal probes to study the formation and evolution of large scale structures and galaxies in the universe. A 10-m class ground based telescope, X-ray observatories (Chandra, XMM-Newton) and HST/ACS are allowing us to perform an unprecedented study of distant massive clusters of galaxies in the redshift range $0.84 < z < 1.3$, selected from X-rays surveys. In this paper we summarize our results on the structure and dynamics of two of these clusters derived from imaging and spectroscopic data as well as our results on the evolution of early-type galaxies.

Keywords: Clusters of Galaxies; Galaxy Cluster Structure; Galaxy Evolution.

PACS Nos.: 98.65.Cw, 98.65.Hb, 98.62.Ai, 98.62.Py, 98.62.Lv, 98.80.Es

1. Introduction

Clusters of galaxies are the largest gravitationally bound structures known in the universe, constituting a collection of galaxies embedded in a hot ($T \sim 10^7$ - 10^8 K) and thin ($n_e \sim 10^{-3} \text{ cm}^{-3}$) gas in the gravitational potential created by the cluster dark matter (DM) halo. The velocity dispersion of galaxies in clusters is typically $\sigma_v \sim 800$ - 1000 km s^{-1} . The scale of a cluster of galaxies is of the order of a few Mpc, and its mass can vary between 10^{14} and $10^{15} M_\odot$.

Clusters of galaxies are fundamental objects in modern cosmology. They represent regions where mass overdensities have reached maximum amplitudes; consequently, the study of their correlation in space can be used to estimate the power spectrum of density fluctuations in the universe. The mass function of distant galaxy clusters is sensitive to the cosmological parameters defining the geometry and dynamics of the universe^{1,2,3}, therefore galaxy clusters can be used to probe the cosmological model. Moreover, galaxy clusters are ideal laboratories to study the effects of environment on the formation and evolution of galaxies, in particular of

2 *R. Demarco, P. Rosati & H. C. Ford*

early-type galaxies, the most massive galaxies known. Predictions of the spectrophotometric properties of early-type galaxies in clusters based on hierarchical models of galaxy formation^{4,5,6} differ significantly at redshifts $z \gtrsim 1$ from models in which ellipticals formed at high redshift in a monolithic collapse.⁷ A detailed analysis of the internal structure and dynamics of galaxy clusters is thus essential to understand their formation and evolution as well as the formation and evolution of their baryon content (galaxies and gas).

In this context, we have undertaken an ambitious observational program to obtain high angular resolution imaging with the Advanced Camera for Surveys (ACS)⁸ on the HST of 7 clusters of galaxies⁹ with redshift in the range $0.8 < z < 1.3$. The aim of this program is to study the formation and evolution of clusters and their galaxy populations. These data are supported by other space and ground based observations covering a wide range in wavelength, from X-rays to near-IR. As an example of our program, in this paper we review our panchromatic study of two of these clusters, which are among the most distant ($z \gtrsim 1$) massive clusters of galaxies known today: RX J0152.7-1357 ($z = 0.84$; hereafter RX J0152 for brevity) and RDCS1252.9-2927 ($z = 1.24$; hereafter RDCS J1252 for brevity). Multi-wavelength imaging data and optical spectroscopy are combined to provide detailed information about the structure of these clusters and the spectrophotometrical properties of their galaxy populations. Throughout this paper, unless otherwise indicated, we assume a Λ CDM cosmology with $H_0 = 70 \text{ kms}^{-1} \text{ Mpc}^{-1}$, $\Omega_m = 0.3$ and $\Omega_\Lambda = 0.7$.

2. Physics of galaxy clusters

Multi-wavelength observations of galaxy clusters are fundamental tools to examine the physical properties of their components: DM and Baryons (gas and galaxies). DM contributes $\sim 85\%$ of the cluster mass while the remaining mass comes mostly from the gas. Galaxies represent a tiny fraction ($\sim 1\%$) of the cluster mass. Optical and near-IR observations allow us to study the physics of cluster galaxies and X-ray observations show us the physical properties of the intracluster medium (ICM) gas.

Clusters of galaxies are among the strongest sources of X-rays with typical X-ray luminosities of $L_X \sim 10^{43} - 10^{45} \text{ ergs s}^{-1}$, which makes them detectable at redshifts beyond unity. This emission is due to thermal Bremsstrahlung from the interaction between the electrons and ions of the hot ICM. In a local thermodynamical equilibrium state at temperature T , the X-ray emissivity of the ICM, in units of $W \text{ m}^{-3} \text{ Hz}^{-1}$, is¹⁰:

$$\epsilon_\nu(\mathbf{r}) = 5.44 \times 10^{-52} \overline{Z^2} n_e(\mathbf{r}) n_i(\mathbf{r}) T^{-1/2}(\mathbf{r}) g^{ff}(Z, T(\mathbf{r}), \nu) e^{-h\nu/(kT(\mathbf{r}))}, \quad (1)$$

where $n_e(\mathbf{r})$ is the electron number density, $n_i(\mathbf{r})$ is the ion number density and $\overline{Z^2}$ is the mean-square atomic charge on the ions. The coefficient $g^{ff}(Z, T(\mathbf{r}), \nu)$ is a correcting factor, called the Gaunt factor.^{11,12} This equation can be fit to the observed X-ray spectrum to estimate the ICM temperature and metallicity and,

since Eq. (1) depends on the square of the gas density ($\rho_{gas}^2 \propto n_e^2 \propto n_e n_i$), a model for ρ_{gas} can be used to fit the cluster X-ray surface brightness and obtain the gas distribution. A popular description for the density profile of an iso-thermal gas in hydrostatic equilibrium is the β -model¹³:

$$\rho_{gas}(r) = \rho_0 \left\{ 1 + \left(\frac{r}{r_c} \right)^2 \right\}^{-3\beta/2}. \quad (2)$$

The parameter β is the ratio between kinetic galaxy energy and thermal gas energy: $\beta = (\mu m_p \sigma_v^2)/(k_B T)$, where σ_v is the galaxy velocity dispersion along the line of sight. Once the temperature is known and assuming that the cluster gas is in hydrostatic equilibrium, then the cluster mass distribution is given by:

$$M(< r) = -\frac{k_B r}{\mu m_p G} T \left\{ \frac{d \log \rho_{gas}(r)}{d \log r} + \frac{d \log T(r)}{d \log r} \right\}. \quad (3)$$

This mass, obtained from X-ray observations, can be compared with other mass estimates, such as the virial mass and the gravitational lensing mass. Spectroscopic observations in the optical of cluster galaxies allow us to measure the galaxy velocity dispersion along the line of sight, σ_v . Once the projected cluster galaxy positions are obtained from the imaging data, the virial mass of the cluster can be computed as¹⁴:

$$M_V = \frac{3\pi \sigma_v^2}{2 G} \left(\frac{N(N-1)}{\sum_{i>j} R_{ij}^{-1}} \right), \quad (4)$$

where N is the number of galaxies and R_{ij} is the distance between any pair of galaxies. Since the velocity dispersion σ_v is dependent on the dynamical state of the cluster, Eq. (4) provides a true estimate of the cluster mass only if the structure is relaxed. In cases where the cluster structure is not in virial equilibrium, Eq. (4) represents an upper limit to the cluster mass. In contrast, the weak lensing analysis¹⁵ offers a way of estimating masses which is independent of the cluster dynamical state. However, weak lensing turns out to be sensitive to the distribution of matter along the line of sight as well as to the distribution of background sources. Therefore, a good knowledge of these distributions is required to obtain reliable mass estimates. The strong lensing technique¹⁵ is a more robust mass tracer; however, it requires the existence of gravitational arcs in the cluster field, which are not always present or detectable, and a knowledge of their redshifts.

Assuming that clusters of galaxies are in a relaxed state and that gravity is the only dominant driver of evolution, theory shows that these objects are self-similar structures described by scaling relations relating mass, temperature and luminosity. In particular, if the gas fraction in clusters is independent of temperature, then a relation $L_x \propto T^2$ is expected. Observational evidence shows, however, that local

4 *R. Demarco, P. Rosati & H. C. Ford*

clusters follow a relation $L_x \propto T^\alpha$, with $\alpha > 2$. Although some analyses indicate a value of α independent of temperature^{16,17}, there is observational evidence that points toward larger values of α on group scales making the $L_x - T$ relation even steeper at lower temperatures ($T \lesssim 1$ keV).¹⁸ A departure from theoretical predictions is also shown by the observed $L_x - M$ and $T - M$ relations.^{19,20} The departure from self-similarity of the $L_x - T$ relation suggests that energy injection from non-gravitational processes^{21,22,23,24} or a temperature dependent gas fraction may be the cause of the departure from theory, although the latter is likely not the case.²⁵ When observing clusters or groups of galaxies at higher redshifts (up to $z \sim 1$), the behavior of the $L_x - T$ relation shows no major change.²⁶ This together with a non evolving ICM metallicity of about $0.3 Z_\odot$ ^{27,28}, since $z \sim 1$ down to the local universe, suggest an early formation epoch for the ICM with the major episode of metal enrichment and gas preheating occurring at $z > 1$. With the development of more advanced techniques, detailed hydrodynamical simulations²⁹ of cluster formation including galaxy feedback are being performed in order to reproduce the observations, casting more light on the above issues and deepening our understanding of cluster formation.

In the optical range, spectroscopic and imaging observations of cluster galaxies provide us with valuable information about the dynamics of the cluster itself and the properties of the member galaxies. Spectrophotometric surveys are essential in determining the overall galaxy Luminosity Function (LF) of clusters, a powerful tool for constraining models of galaxy formation and evolution. The LF is commonly modeled with a Schechter function³⁰:

$$\phi(L) = \frac{\phi^*}{L^*} \left(\frac{L}{L^*} \right)^{-\alpha} e^{-(L/L^*)}, \quad (5)$$

where L^* is the characteristic luminosity of the population of galaxies and corresponds to the luminosity over which the exponential term dominates, i.e., the bright end of the LF. The index α gives the slope of the power law behavior of the LF at low luminosities, and the normalization ϕ^* determines the volume density of sources n_0 as $n_0 = \int_0^\infty \phi(L) dL = \phi^* \Gamma(1 - \alpha)$. Observations of the galaxy LF in clusters over a wide range in redshift ($0 < z \lesssim 1$)^{31,32} show compelling evidence for the evolution of bright (massive) galaxies in clusters that is consistent with pure passive evolution models with $z_f \gtrsim 2$. If merging plays a role in the formation of these galaxies, these results suggest that any merging activity should take place at higher redshift. The same conclusion is obtained from the LF of field galaxies³³, showing that massive elliptical galaxies were already in place at $z \simeq 1$, forming their stars and assembling their mass at higher redshift. Passive evolution models of early-type galaxies in clusters also show a good agreement with photometric observations of cluster galaxies. The color-magnitude (CM) diagram of clusters shows a well defined red sequence, the locus formed by the majority of red early-type cluster galaxies. The tight CM relation observed in local^{34,35} and distant^{36,37,38,39,40} cluster early-type galaxies indicates that in clusters these galaxies are formed at redshifts $z \gtrsim 2$, after an initial

burst of star formation followed by pure luminosity evolution, posing difficulties for hierarchical models that have “late” ($z < 2$) formation of the brightest galaxies. In addition, spectroscopic observations of cluster galaxies allow us to explore their stellar content, thus providing essential information to better constrain galaxy evolution models of galaxies and understand the galaxy-ICM connection during the cluster evolution.

3. The observational data

As an example of our cluster program, in this paper we present a summary of results obtained so far from our multi-wavelength study of two distant clusters RX J0152 at $z = 0.837$ ⁴² and RDCS J1252 at $z = 1.237$ ²⁶, both selected from the Rosat Deep Cluster Survey (RDCS)⁴³. In addition to the ACS data, they have also been targeted for X-ray (Chandra and XMM-Newton satellites) and optical and near-IR (ESO NTT and ESO VLT) observations as well as for optical spectroscopy (ESO VLT). The ground based optical and near-IR imaging as well as the VLT spectroscopic survey of RX J0152 are presented in Demarco et al. (2005).⁴⁴ ACS observations of the same cluster are discussed and analysed in Blakeslee et al. (in preparation), Homeier et al. (2005)⁴⁵, and Jee et al. (2005)⁴⁶ and the X-ray observations are presented in Maughan et al. (2003).⁴⁷ In the case of RDCS J1252, very deep near-IR imaging with VLT/ISAAC⁴⁸ was obtained in very good seeing (< 0.5) conditions allowing us to reach a limiting magnitude (5σ detection threshold over a $0''.9$ diameter aperture) in the Vega system of 25.6 and 24.1 in the J- and K_s -bands respectively. X-ray observations of RDCS J1252 are described in Rosati et al. (2004)²⁶ and the ACS observations of this cluster are presented in Blakeslee et al. (2003)⁴⁰ and Holden et al. (2005).⁴¹

Table 1. Physical properties of RX J0152.7-1357 and RDCS J1252.9-2927. Redshift and velocity dispersion values are from Demarco et al. 2004, 2005 and Demarco et al. 2005, in preparation. Temperatures, X-ray luminosities and metallicities are from Ettori et al. 2004.

Cluster	z	Temperature (keV)	X-ray L_{bol} $\times 10^{44}$ (ergs s ⁻¹)	Rest Frame Vel. Disp. (km s ⁻¹)	Metallicity (Z_{\odot})
RX J0152.7-1357 N	0.839	$6.0^{+1.1}_{-0.7}$	10.67 ± 0.67	919 ± 168	$0.17^{+0.19}_{-0.16}$
RX J0152.7-1357 S	0.830	$6.9^{+2.9}_{-0.8}$	7.73 ± 0.40	737 ± 126	< 0.22
RDCS J1252.9-2927	1.237	$6.0^{+0.7}_{-0.5}$	6.6 ± 1.1	766 ± 89	$0.36^{+0.12}_{-0.10}$

4. The galaxy cluster RX J0152 ($z=0.837$)

RX J0152 is a massive dynamically young system at $z = 0.837$ where two clusters of galaxies are likely merging. Since its discovery with ROSAT⁴², a number of observations in the X-ray domain as well in the optical have been carried out, confirming its complex structure and unvirialized state.^{47,46,44,45}

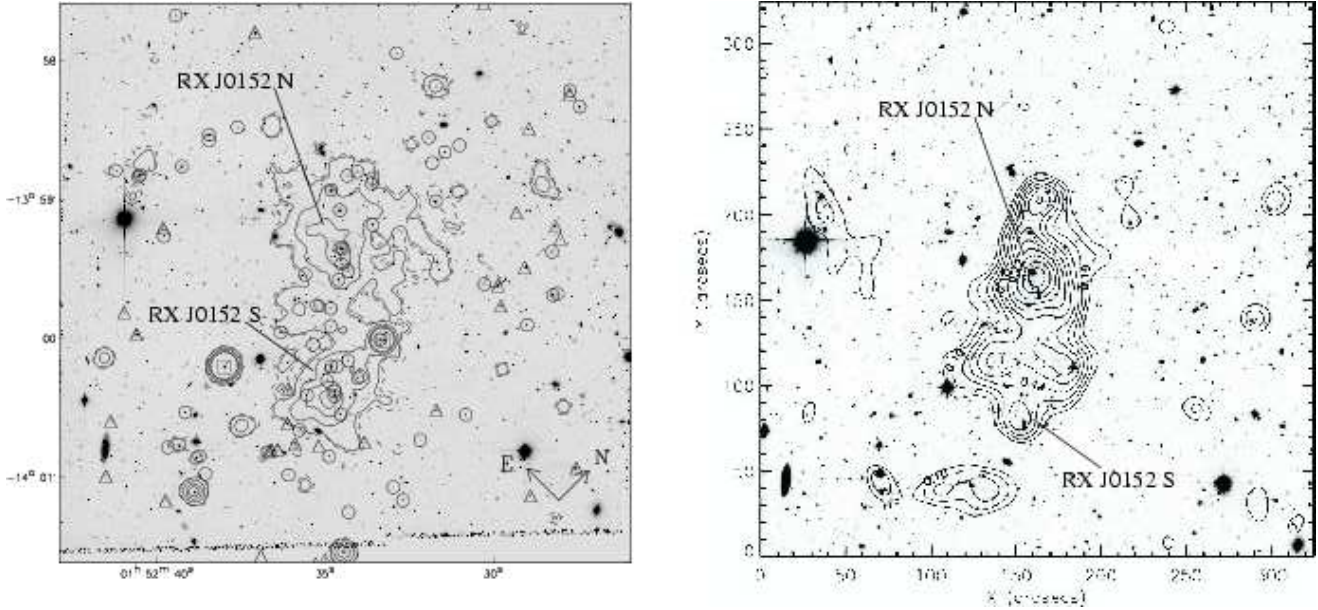


Fig. 1. RX J0152. **Left:** Chandra X-ray iso-contours overlaid on the ACS optical image. The circles are spectroscopically confirmed “passive” (no emission lines) cluster members, the triangles are confirmed star-forming galaxies, and the two squares at the centers of two X-ray point sources are confirmed cluster Seyferts (Demarco et al. 2005). **Right:** Mass iso-contours from the weak lensing analysis (Jee et al. 2005) overlaid on the ACS optical image (Figure taken from Jee et al. [2005]).

4.1. *RX J0152: Cluster structure and dynamics*

Fig. 1 shows the distribution of Baryons and DM in RX J0152. The X-ray data from Chandra (Fig. 1-Left) clearly shows that RX J0152 is composed of two extended central substructures; the centroids of these two substructures (subclusters) are separated by $1'.6$ (730 kpc at the cluster redshift) on the sky. The main physical characteristic of these two subclusters called RX J0152 N and RX J0152 S are given in table 1. A third extended substructure is also observed at about 1 Mpc to the East of the two central ones, associated with a galaxy overdensity.

The X-ray analysis^{47,49} provides evidence of a possible merger in progress between the two main subclusters. VLT/FORS spectroscopic observations⁴⁴ have allowed us to confirm the complex structure observed in the X-rays and giving further support to the merger hypothesis. The distribution of spectroscopically confirmed cluster members presents galaxy overdensities which coincide with the location of the three main X-ray extended regions. The velocity dispersion of spectroscopic members belonging to RX J0152 N and RX J0152 S are given in table 1. These values, when compared to the corresponding temperatures of the same substructures, are in good agreement with the observed σ -T relation, indicating that RX J0152 N and S are likely two clusters in a dynamical state close to virialized. Their masses

are estimated to be $(2.5 \pm 0.9) \times 10^{14} M_{\odot}$ and $(1.1 \pm 0.4) \times 10^{14} M_{\odot}$ for RX J0152 N and S respectively.⁴⁴

The main substructures detected in the ICM and galaxy distribution are also recovered by weak lensing analyses of the cluster,⁴⁶ as shown in Fig. 1-Right, which confirm that most of the baryon (ICM and galaxies) content is in the potential well created by the DM distribution. The observed offsets between the centroids of the gas, galaxy and DM distributions of the three main substructures are consistent with the picture in which RX J0152 is still in the process of assembling its mass through the accretion/merging of substructures.⁴⁶ Assuming that the two main sub-clusters are coming together for the first time and considering their projected separation and relative velocity, the required time to first crossing is estimated to be $\Delta t_c \simeq 0.4$ Gyr. This time implies that the virialization of the cluster as a whole will begin at a redshift $z_c \simeq 0.75$.

Because of the non-uniform distribution of the baryons and DM, the overall structure of the cluster is likely not to be in virial equilibrium. Indeed, the overall velocity dispersion of the cluster turns out to be too high to be consistent with the observed σ -T relation.⁴⁴ Therefore, an accurate estimate of the virial mass of the whole cluster, based on the velocity distribution of spectroscopic cluster members, is not possible.

4.2. RX J0152: Galaxy populations

The spectroscopic survey carried out with the VLT allowed us to obtain spectra for 102 cluster members.⁴⁴ We use these spectra to separate cluster members in two groups: galaxies with emission lines (star-forming galaxies) and galaxies without emission line features (passive galaxies). Passive galaxies and star-forming galaxies are indicated by small circles and triangles respectively in Fig. 1-Left. One striking feature is that all the star-forming galaxies are distributed in the outskirts of the cluster, avoiding the high density regions traced by the X-ray emission^{44,45} (see Fig. 1-Left). The derived star-formation rate (SFR) of these galaxies⁴⁵ turns out to be smaller than that of galaxies in the field environment. A simple interpretation for this is that galaxies at large radii from the cluster center are falling into the cluster potential, suppressing their star-forming activity as they interact with the ICM (see Homeier et al. 2005).⁴⁵

An analysis of the ground based⁴⁴ and ACS (Blakeslee et al., in prep.) photometry of this cluster shows a clear CM relation in the corresponding CM diagram. The locus of the CM relation is mainly defined by passive galaxies, although a few emission line galaxies are also observed in this region of the diagram. By comparing these data to models^{50,51} we find that passive cluster galaxies have colors consistent with passive evolution of early-type galaxies formed at $z \gtrsim 2$.

The few emission line galaxies observed within 1σ from the best fit of the locus of the CM relation have colors as red as passive early-type (elliptical) galaxies. This suggests the existence of an old stellar population inhabiting these galaxies,

although intrinsic dust extinction may also be the cause of the observed reddening. The ACS images reveal that most of these galaxies indeed have a red bulge structure in the center surrounded by a bluer disk, where the star-forming activity should be taking place. A more detailed analysis of the spectroscopic data shows that some of these red star-forming galaxies are also hosts of a young (~ 1 Gyr old) stellar population (see Demarco et al. [2005]⁴⁴ for a more detailed discussion). The fact that these galaxies harbor stellar population of different ages raises the interesting possibility that these objects may be undergoing a transition stage between late-type field galaxies falling into the cluster and early-type passive galaxies located in the cluster core. Galaxy-ICM interactions may play a considerable role in this transition phase.

5. The galaxy cluster RDCS J1252 ($z=1.237$)

RDCS J1252 is one of the most X-ray luminous cluster discovered to date at $z > 1$.²⁶ Its main physical properties are summarized in table 1. Extensive spectroscopy with the VLT has confirmed its redshift to be $z = 1.237$. This cluster is among the three clusters at $z > 1.2$ observed with the ACS⁹ and is providing fundamental information to understand cluster formation and galaxy evolution. The main results to date are reviewed in the following sections.

5.1. *RDCS J1252: Cluster structure and dynamics*

The X-ray extended emission of RDCS J1252 is in clear contrast, in terms of spatial distribution, to that of RX J0152. The X-ray iso-contours shown in Fig. 2-b are those from Chandra. The more uniform distribution of the cluster X-ray emission, compared to that of RX J0152, suggests that the ICM is in a more advanced state of relaxation, implying that it had to be assembled at higher redshift. However, when looking at it in more detail, a coma-like asymmetry in the East-West direction on the sky of the X-ray isophotes (Fig. 2-b) suggests the possibility that the ICM has been affected by a recent merging episode. Interestingly, the spatial distribution of the cluster K-band ($2.2 \mu\text{m}$) luminosity weighted light distribution (Fig. 2-c) from photometric members (including spectroscopic ones) shows a similar elongated structure.^{52,53} The elongation of the cluster is confirmed by the weak lensing analysis of the cluster that finds a similar East-West elongation in the DM distribution⁵⁴ (Fig. 2-a). The cluster core, as seen by the ACS, is shown in Fig. 2-d.

We derived the cluster luminosity, ICM temperature and metallicity from the X-ray data²⁶, while the spectroscopic data allowed us to securely identify cluster galaxies and thus determine the cluster velocity dispersion (see table 1). The comparison of these measurements with those of clusters at lower redshift allow us to study the evolution of scaling relations from $z = 1.24$ down to the local universe. The ICM temperature and velocity dispersion of RDCS J1252 are in good agreement with the observed $\sigma - T$ relation while the X-ray luminosity, entropy (S) and temperature values suggest only a mild positive evolution of the $L_x - T$ and

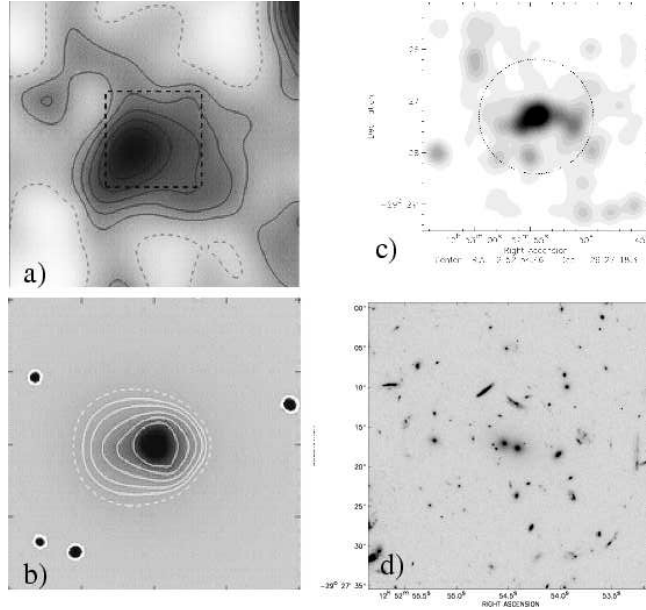


Fig. 2. RDCS J1252. **a)** ACS weak lensing mass map (taken from Lombardi et al. 2005) centered on the optical center of the cluster and covering 5.7×5.7 arcmin². The dashed square has a side length of 2 arcmin (1 Mpc at the cluster redshift). **b)** Chandra X-ray iso-contours in the central 2 arcmin of the cluster (dashed square; taken from Lombardi et al. 2005). **c)** Map of the smoothed K-band light of photometric member galaxies. The circle marks the central 130 arcseconds diameter region of the cluster; taken from Toft et al. (2004). **d)** The 0.6×0.6 arcmin² ACS optical image of the cluster core, dominated by two elliptical galaxies. In all panels North is up and East is left. The distributions of DM, gas and cluster members (K-band light) are elongated in the East-West direction.

$S - T$ relations.²⁵ RDCS J1252 appears thus well thermalized with thermodynamical properties similar to those of clusters at low redshift. The value of the metallicity obtained from the XMM spectroscopic data²⁶ turns out to be consistent with the mean ICM metallicity value for lower redshift clusters.²⁸ This result thus provides further support for the lack of evolution of the amount of metals in galaxy clusters up to $z \simeq 1.3$ and is consistent with the major episode of metal enrichment occurring at ~ 3 . The total mass of the cluster is estimated to be $(1.9 \pm 0.3) \times 10^{14} M_{\odot}$ within a radius of 536 kpc,²⁶ consistent with the $\sigma - M$ relation predicted by Bryan & Norman (1998).⁵⁵ In general, the structure and physical properties of RDCS J1252's ICM show that this cluster is a massive system in an advanced thermodynamical state, with scale properties similar to those of clusters at low redshift, that we are observing at a lookback time of 8.5 Gyrs (when the universe was about 36% of its present age).

5.2. RDCS J1252: Galaxy populations

So far a total of 38 cluster members have been spectroscopically confirmed with VLT/FORS (Demarco et al., in prep.). Like RX J0152, star-forming galaxies are preferentially located in the outer (infalling) regions of the cluster, with passive early-type galaxies to dominate the cluster center.

The high angular resolution of the ACS allows us to examine in detail the morphology of cluster galaxies even at such a large lookback time (Rosati et al., in preparation). One interesting feature is that, while all the passive member galaxies are well characterized by an early-type appearance (bulge-like structure), only one of the star-forming cluster members shows a well defined morphology with grand design spiral arms or a disk structure surrounding a central bulge. Most of these galaxies look quite irregular, suggesting that they may be still forming. This is in contrast to RX J0152, where many star-forming galaxies can be clearly classified as spiral galaxies. More generally speaking, and excluding passive galaxies, the comparison of galaxy morphologies between RX J0152 and RDCS J1252 suggests that galaxy formation is still on-going at $z \sim 1.2$ and that Hubble-type spirals may not be established until $z \lesssim 1$. However, more observations of high- z galaxies are needed to strengthen this conclusion.

The combination of ground based spectroscopy with near-IR imaging from VLT has allowed us to compute the K-band galaxy LF of the cluster⁵³ which, at the redshift of $z = 1.24$, allows us to probe the rest-frame z -band light from the cluster. When comparing the derived LF with the z -band LF of galaxy clusters in the local universe a non evolution of the shape of the bright end of the LF is observed, indicating that massive elliptical galaxies which dominate the bright end of the galaxy LF were already in place at $z = 1.24$. Another important observation is the brightening of M^* (the characteristic magnitude associated with L^*) compared to lower redshift clusters. This finding is in agreement with the result from previous work³¹ indicating that galaxies in clusters become brighter at higher redshifts.

The same ground based near-IR data⁴⁸ and ACS optical data⁴⁰ have been used to study the distribution of the cluster galaxy populations in Color-Magnitude space. These studies, both independent, arrive at similar conclusions. A clear and tight CM relation for early-type (passive) galaxies is observed in RDCS J1252 at $z = 1.24$ with a slope and scatter similar to lower redshift values.³⁶ These results thus confirm that the CM relation of cluster early-type is a metallicity-mass relation instead of an age-mass relation, i.e., more massive (luminous) early-type galaxies are able to better retain metals and thus to produce redder colors.⁵⁰ Although the scatter in colors of the early type galaxies permits considerable variation in the ages, their mean luminosity weighted age is quite old, corresponding to $z_f \sim 3$.

Both CM studies and the K-band galaxy LF of RDCS J1252 also indicate that massive early-type galaxies evolved passively in luminosity since their epoch of formation. The above results for early-type galaxies in RDCS J1252 are in agreement with studies of early-type galaxies in the field³³ and pose challenging problems to

hierarchical models of galaxy formation. However, despite the fact that early-type galaxies in RDCS J1252 are home for stars with a mean age of approximately 2.7 Gyrs,⁴⁸ the spectroscopic data available suggest an interesting new result. When combining the spectra of the 10 brightest spectroscopic members, a prominent H δ feature emerges.⁵⁶ This balmer absorption line indicates the presence of young A- and F-type stars, born about 1 Gyr previous to the epoch of observation. Although a quantitative analysis is needed to confirm this result, this observation would indicate that most luminous early-type galaxies in RDCS J1252 host young (post-starburst) stellar populations produced in recent episodes of star formation at $z \lesssim 2$. We would be thus approaching the formation epoch of these galaxies as we observe traces of their latest star-forming episode.

6. Conclusions

The unprecedented panchromatic study carried out so far on two of the most distant clusters of galaxies known to date is providing us with crucial information to better understand cluster evolution and the formation and evolution of luminous early-type galaxies, the most massive galaxies known. The main conclusions can be summarized as follows. Scaling relations such as the L_x -T relation and ICM metallicity do not significantly evolve up to $z = 1.24$ pushing energy injection processes and metal production in galaxy clusters to $z \gtrsim 3$. The analysis of the CM relation in RDCS J1252 at $z = 1.24$ provides valuable information to understand the formation and evolution of massive elliptical galaxies. These galaxies would have formed the bulk of their stars at $z \sim 3$ (when the universe was $\sim 15\%$ of its present age) evolving passively in luminosity since then. The large lookback time of formation of massive (luminous) early type galaxies and their passive evolution are consistent with the results from galaxy LF studies in cluster and field environments. Furthermore, these studies support the simple model of monolithic collapse for the formation of elliptical galaxies. In particular, the LF of galaxies in the field³³ suggests that most of the merging which form elliptical galaxies in the hierarchical models should occur at redshift $z > 2 - 3$. This study poses difficulties for hierarchical models which underpredict the density of luminous galaxies at $z \geq 1$ and overpredict significantly the density of low luminosity galaxies at $z \leq 1$.

In addition to all the above, the joint analysis of the available data on all the clusters observed with the ACS is providing more robust and statistically significant information about the structure and evolution of clusters and cluster galaxies. In particular, the morphology-density relation^{57,58} is well established at $z \sim 1$, an epoch when the universe was $\sim 40\%$ its present age. Late-type star-forming galaxies are observed to prefer the outer low density regions of clusters, while early-type passive galaxies populate the high density regions of the cluster cores. Interesting evolutionary trends are observed in the morphology-density relation as a function of density and redshift⁵⁹. The available data suggest that this evolution is primarily driven by evolution in the fraction of S0 and Spiral+Irregular galaxies: a deficit of

12 *R. Demarco, P. Rosati & H. C. Ford*

S0s and an excess of Spiral+Irregular galaxies are observed at $z \sim 1$ relative to the local galaxy population.⁵⁹ Moreover, mild correlations of the cluster early-type fraction and cluster star-formation rate with cluster X-ray luminosity have been detected.^{59,45}

In the future, the integration of the Spitzer/IRAC data available on the clusters in the ACS cluster program will provide new information about the bulk of the stellar mass in galaxies (whose light peaks at about $2 \mu\text{m}$ rest frame) at redshifts $z \gtrsim 1$. Also, the strong lensing analysis of some of the clusters observed with the ACS will allow us to accurately model the mass distribution in the central regions of distant clusters, thus providing important tests of the Cold Dark Matter (CDM) paradigm. In addition to the recent discovery of an X-ray luminous cluster at $z = 1.4$,⁶⁰ more clusters at similar and higher redshift need to be discovered in order to bridge the evolutionary gap between our most distant clusters and their likely progenitors, the so called proto-clusters which have been discovered at redshifts $z \geq 2$.^{61,62}

Acknowledgments

ACS was developed under NASA contract NAS5-32865. We thank our fellow ACS team members for their important contributions to this research and we also thank the support from ESO staff in Chile and Germany. We are grateful to Ken Anderson, John McCann, Sharon Bushing, Alex Framarini, Sharon Barkhouser, and Terry Allen for their invaluable contributions to the ACS project at JHU. This investigation has been partially supported by NASA grant NAG5-7697.

References

1. Bahcall, N. A. & Cen, R. 1993, ApJL, 407, L49
2. Bahcall, N. A., Fan, X., & Cen, R. 1997, ApJL, 485, L53
3. Fan, X., Bahcall, N. A., & Cen, R. 1997, ApJL, 490, L123
4. Kauffmann, G. 1996, MNRAS, 281, 487
5. Kauffmann, G. & Charlot, S. 1998a, MNRAS, 294, 705
6. Kauffmann, G. & Charlot, S. 1998b, MNRAS, 297, L23
7. Eggen, O. J., Lynden-Bell, D., & Sandage, A. R. 1962, ApJ, 136, 748
8. Ford, H. C., et al. 2002, Proc. SPIE, 4854, 81
9. Ford, H., et al. 2004, ArXiv Astrophysics e-prints, astro-ph/0408165
10. Binney, J. & Merrifield, M. 1998, Galactic astronomy. Princeton, NJ : Princeton University Press (Princeton series in astrophysics)
11. Karzas, W. J. & Latter, R. 1961, ApJS, 6, 167
12. Kellogg, E., Baldwin, J. R., & Koch, D. 1975, ApJ, 199, 299
13. Cavaliere, A. & Fusco-Femiano, R. 1976, A&A, 49, 137
14. Girardi, M., Giuricin, G., Mardirossian, F., Mezzetti, M., & Boschin, W. 1998, ApJ, 505, 74
15. Mellier, Y. 1999, ARA&A, 37, 127
16. Mulchaey, J. S. & Zabludoff, A. I. 1998, ApJ, 496, 73
17. Osmond, J. P. F. & Ponman, T. J. 2004, MNRAS, 350, 1511
18. Helsdon, S. F. & Ponman, T. J. 2000, MNRAS, 315, 356

19. Sanderson, A. J. R., Ponman, T. J., Finoguenov, A., Lloyd-Davies, E. J., & Markevitch, M. 2003, *MNRAS*, 340, 989
20. Finoguenov, A., Reiprich, T. H., & Böhringer, H. 2001, *A&A*, 368, 749
21. Lloyd-Davies, E. J., Ponman, T. J., & Cannon, D. B. 2000, *MNRAS*, 315, 689
22. Balogh, M. L., Babul, A., & Patton, D. R. 1999, *MNRAS*, 307, 463
23. Tozzi, P. & Norman, C. 2001, *ApJ*, 546, 63
24. Borgani, S., Governato, F., Wadsley, J., Menci, N., Tozzi, P., Lake, G., Quinn, T., & Stadel, J. 2001, *ApJL*, 559, L71
25. Ettori, S., Tozzi, P., Borgani, S., & Rosati, P. 2004, *A&A*, 417, 13
26. Rosati, P., et al. 2004, *AJ*, 127, 230
27. Renzini, A. 1997, *ApJ*, 488, 35
28. Tozzi, P., Rosati, P., Ettori, S., Borgani, S., Mainieri, V., & Norman, C. 2003, *ApJ*, 593, 705
29. Borgani, S., et al. 2004, *MNRAS*, 348, 1078
30. Schechter, P. 1976, *ApJ*, 203, 297
31. de Propriis, R., Stanford, S. A., Eisenhardt, P. R., Dickinson, M., & Elston, R. 1999, *AJ*, 118, 719
32. Ellis, S. C. & Jones, L. R. 2004, *MNRAS*, 348, 165
33. Pozzetti, L., et al. 2003, *A&A*, 402, 837
34. Bower, R. G., Lucey, J. R., & Ellis, R. S. 1992, *MNRAS*, 254, 601
35. Terlevich, A. I., Caldwell, N., & Bower, R. G. 2001, *MNRAS*, 326, 1547
36. Stanford, S. A., Eisenhardt, P. R., & Dickinson, M. 1998, *ApJ*, 492, 461
37. Rosati, P., Stanford, S. A., Eisenhardt, P. R., Elston, R., Spinrad, H., Stern, D., & Dey, A. 1999, *AJ*, 118, 76
38. van Dokkum, P. G., Stanford, S. A., Holden, B. P., Eisenhardt, P. R., Dickinson, M., & Elston, R. 2001, *ApJL*, 552, L101
39. Stanford, S. A., Holden, B., Rosati, P., Eisenhardt, P. R., Stern, D., Squires, G., & Spinrad, H. 2002, *AJ*, 123, 619
40. Blakeslee, J. P., et al. 2003, *ApJL*, 596, L143
41. Holden, B. P., et al. 2005, *ArXiv Astrophysics e-prints*, arXiv:astro-ph/0503365
42. Della Ceca, R., Scaramella, R., Gioia, I. M., Rosati, P., Fiore, F., & Squires, G. 2000, *A&A*, 353, 498
43. Rosati, P., Della Ceca, R., Norman, C., & Giacconi, R. 1998, *ApJL*, 492, L21
44. Demarco, R., et al. 2005, *A&A*, 432, 381
45. Homeier, N. L., et al. 2005, *ApJ*, 621, 651
46. Jee, M. J., White, R. L., Benítez, N., Ford, H. C., Blakeslee, J. P., Rosati, P., Demarco, R., & Illingworth, G. D. 2005, *ApJ*, 618, 46
47. Maughan, B. J., Jones, L. R., Ebeling, H., Perlman, E., Rosati, P., Frye, C., & Mullis, C. R. 2003, *ApJ*, 587, 589
48. Lidman, C., Rosati, P., Demarco, R., Nonino, M., Mainieri, V., Stanford, S. A., & Toft, S. 2004, *A&A*, 416, 829
49. Huo, Z., Xue, S., Xu, H., Squires, G., & Rosati, P. 2004, *AJ*, 127, 1263
50. Kodama, T. & Arimoto, N. 1997, *A&A*, 320, 41
51. Bruzual A., G. & Charlot, S. 1993, *ApJ*, 405, 538
52. Demarco, R., Rosati, P., Lidman, C., Nonino, M., Mainieri, V., Stanford, A., Holden, B., & Eisenhardt, P. 2004, *Clusters of Galaxies: Probes of Cosmological Structure and Galaxy Evolution, from the Carnegie Observatories Centennial Symposia*. Carnegie Observatories Astrophysics Series. Edited by J.S. Mulchaey, A. Dressler, and A. Oemler, 2004. Pasadena: Carnegie Observatories, <http://www.ociw.edu/ociw/symposia/series/symposium3/proceedings3.html>

14 *R. Demarco, P. Rosati & H. C. Ford*

53. Toft, S., Mainieri, V., Rosati, P., Lidman, C., Demarco, R., Nonino, M., & Stanford, S. A. 2004, *A&A*, 422, 29
54. Lombardi, M., et al. 2005, *ApJ*, 623, 42
55. Bryan, G. L. & Norman, M. L. 1998, *ApJ*, 495, 80
56. Rosati, P. 2004, *Clusters of Galaxies: Probes of Cosmological Structure and Galaxy Evolution*, from the Carnegie Observatories Centennial Symposia. Published by Cambridge University Press, as part of the Carnegie Observatories Astrophysics Series. Edited by J.S. Mulchaey, A. Dressler, and A. Oemler, 2004, p. 72.
57. Dressler, A. 1980, *ApJ*, 236, 351
58. Goto, T., Yamauchi, C., Fujita, Y., Okamura, S., Sekiguchi, M., Smail, I., Bernardi, M., & Gomez, P. L. 2003, *MNRAS*, 346, 601
59. Postman, M., et al. 2005, *ApJ*, 623, 721
60. Mullis, C. R., Rosati, P., Lamer, G., Böhringer, H., Schwobe, A., Schuecker, P., & Fassbender, R. 2005, *ApJL*, 623, L85
61. Venemans, B. P., et al. 2002, *ApJL*, 569, L11
62. Miley, G. K., et al. 2004, *Nature*, 427, 47